PHYSICAL REVIEW C **71**, 044901 (2005)

Collective flow of open and hidden charm in Au + Au collisions at $\sqrt{s}$ = 200 GeV

E. L. Bratkovskaya,[1] W. Cassing,[2] H. Stöcker,[1] and N. Xu[3]
[1] *Institut für Theoretische Physik, Universität Frankfurt, D-60054 Frankfurt, Germany*
[2] *Institut für Theoretische Physik, Universität Giessen, D-35392 Giessen, Germany*
[3] *Nuclear Science Division, Lawrence Berkeley National Laboratory, Berkeley, California 94720, USA*
(Received 21 September 2004; published 8 April 2005)

We study the collective flow of open charm mesons and charmonia in Au + Au collisions at $\sqrt{s}$ = 200 GeV within the hadron-string-dynamics (HSD) transport approach. The detailed studies show that the coupling of D, $\bar{D}$ mesons to the light hadrons leads to comparable directed and elliptic flow as for the light mesons. This also holds approximately for J/Ψ mesons since more than 50% of the final charmonia for central and midcentral collisions stem from $D + \bar{D}$ induced reactions in the transport calculations. The transverse momentum spectra of D, $\bar{D}$ mesons and J/Ψ's are only very moderately changed by the (pre-)hadronic interactions in HSD, which can be traced back to the collective flow generated by elastic interactions with the light hadrons.

DOI: 10.1103/PhysRevC.71.044901 PACS number(s): 25.75.−q, 13.60.Le, 14.40.Lb, 14.65.Dw

I. INTRODUCTION

The dynamics of nucleus-nucleus collisions at relativistic heavy ion collider (RHIC) energies are of fundamental interest with respect to the properties of hadronic/partonic systems at high energy densities. Especially, the formation of a quark-gluon plasma (QGP) and its transition to interacting hadronic matter have motivated a large research community for more than two decades [1–4]. However, the complexity of the dynamics has not been unraveled, and the evidence for the formation of a QGP and/or the properties of the phase transition is much debated [5]. Apart from the light and strange flavor (u, $\bar{u}$, d, $\bar{d}$, s, $\bar{s}$) quark physics and their hadronic bound states in the vacuum ($p, n, \pi, K, \phi, \Lambda$, etc.), the interest in hadrons with charm (c, $\bar{c}$) has been rising continuously because the heavy charm quark provides an additional energy scale, which is large compared to $\Lambda_{\rm QCD}$. Accordingly, the hadronic bound states (with a c or $\bar{c}$ quark) have a much larger mass than the ordinary hadrons, and it has been speculated that charmonia ($c\bar{c}$ bound states) especially might only be formed in the very early phase of the heavy ion collision.

In the past, the charmonia J/Ψ, χ_c, and Ψ' have been discussed in context with the phase transition to the QGP since $c\bar{c}$ states might no longer be formed due to color screening [6,7]. However, more recent calculations within lattice QCD (LQCD) have shown that at least the J/Ψ survives up to $\sim$1.5 T_c ($T_c \approx 0.17$ GeV) such that the lowest $c\bar{c}$ states remain bound up to energy densities of about 5 GeV/fm^3 [8–10]. It is presently not clear if the D or D^* mesons also will survive at temperatures above T_c, but strong correlations between a light quark (antiquark) and a charm antiquark (quark) are also likely to persist above T_c.

Moreover, it has been pointed out (within statistical models) that at top RHIC energies the charmonium formation from open charm and anticharm mesons might become essential [11–14] and even exceed the yield from primary nucleon-nucleon (NN) collisions [15]. Such concepts should work out if the early hot and dense medium created in nucleus-nucleus collisions is very strongly interacting and if an approximate chemical equilibrium is achieved rapidly. As argued in Refs. [16–18], an early equilibration might be due to multiparticle interactions on either the partonic [18] or the hadronic side [16,17].

A previous analysis within the hadron-string-dynamics (HSD) transport model [19] demonstrated that the charmonium production from open charm and anticharm mesons becomes essential in central Au + Au collisions at RHIC. This is in accordance with independent studies in Refs. [20,21]. On the other hand, these backward channels—relative to charmonium dissociation with comoving mesons—have been found to be practically negligible at super proton synchroton (SPS) energies. Furthermore, the transport studies in Ref. [22] have shown that chemical equilibrium between the different charmonia J/Ψ, χ_c, Ψ' is not obtained in full phase space on the basis of (pre-)hadronic interactions. As pointed out in [22], this opens up the possibility of distinguishing experimentally a statistical freeze-out concept from an HSD picture.

Apart from the total and relative abundancies of charmonia and open charm mesons, their collective properties are also of interest. Here the transverse momentum (or mass) spectra especially are expected to provide valuable insight to the dynamics in either the very early or late phase [23–27]. We recall that the transverse mass spectra at midrapidity show experimentally a slope parameter that increases ($\sim$linearly) with the hadron mass [28] if the latter involves only light quarks or only a single strange quark. Multistrange baryons indeed show a slope parameter below the linear scaling with mass known from the lighter hadrons [29]. The question thus arises of whether the open charm mesons will follow the trend of the light hadrons similar to kaons (involving only a single s or $\bar{s}$ quark). Also, will the charmonia with their substantially higher mass also show the linear trend as expected from hydrodynamics [23], or do they decouple early as expected in HSD approaches because of the rather low cross sections with light hadrons [27] (cf. also Ref. [25])?

In this work, we extend our previous studies in Refs. [19,22,27] with respect to the collective dynamics of D, $\bar{D}$ mesons and charmonia and concentrate in particular on the transverse mass spectra, the in-plane flow v_1, and the elliptic flow v_2 of these particles. The question we aim at

answering is this: What is the amount of collectivity generated by (pre-)hadronic interactions in the course of the expansion of the system? Any sincere deviation to future measurements thus will indicate additional sources for pressure and/or strong interactions beyond the standard hadron-string picture.

Our study is organized as follows: After a very brief reminder of the conceptional organization of the HSD transport approach in Sec. II, we present the input for the transport calculations with respect to the open charm and charmonium dynamics (or provide the relevent references for details). In Sec. III we present our results for the transverse momentum spectra of D mesons and J/Ψ's for different centralities in Au + Au collisions at $\sqrt{s}$ = 200 GeV. Furthermore, to see the effect of final-state interactions more clearly, we present ratios of momentum spectra from Au + Au reactions relative to scaled pp collisions. Section IV is devoted to the in-plane flow v_1 and elliptic flow v_2 of open charm mesons and charmonia as well as to the freeze-out properties of these particles. Section V concludes this study with a summary.

II. BASIC CONCEPTS OF THE HSD TRANSPORT APPROACH

We employ the HSD transport model [3,30] for our study of Au + Au collisions. This approach takes into account the formation and multiple rescattering of formed hadrons as well as unformed "leading" prehadrons and thus incorporates the dominant final-state interactions. In the transport approach, nucleons, Δ's, N^* (1440), N^* (1535), Λ, Σ and Σ^* hyperons, Ξ's, Ξ^*'s, and Ω's as well as their antiparticles are included on the baryonic side, whereas the 0^- and 1^- octet states are included in the mesonic sector. Inelastic hadron-hadron collisions with energies above $\sqrt{s} \simeq 2.6$ GeV are described by the FRITIOF model [31] (employing PYTHIA v5.5 with JETSET v7.3 for the production and fragmentation of jets [32]), whereas low-energy hadron-hadron collisions are modeled in line with experimental cross sections. We stress that no explicit parton cascading or gluon-gluon dynamics is involved in our transport calculations contrary to, e.g., the multiphase transport (AMPT) model [33] or explicit parton cascades [34].

A systematic analysis of HSD results and experimental data for central nucleus-nucleus collisions from 2A GeV to 21.3A TeV has shown that the spectra for the "longitudinal" rapidity distribution of protons, pions, kaons, antikaons, and hyperons are in reasonable agreement with available data [19,35,36]. However, there are problems with the dynamics in the direction transverse to the beam. Whereas the pion transverse momentum spectra are rather well described from lower alternating-gradient synchroton (AGS) to top RHIC energies, the transverse momentum slopes of kaons/antikaons are clearly underestimated above $\sim$5A GeV in central Au + Au collisions. Reference [36] attributes this failure to a lack of pressure generation in the very early phase of the heavy ion collisions, which also shows up in the underestimation of the elliptic flow of charged hadrons at RHIC energies [19].

We note that the inclusion of initial-state Cronin effects gives a substantial hardening of kaon spectra at RHIC energies, but the slope of the pion spectra at low m_T is only slightly enhanced. In the present study we also included the Cronin effect; however, we found that it has only a small impact on charm and charmonia spectra.

Despite the deficiences pointed out above, the overall reproduction of the experimental hadron spectra is sufficiently realistic that we can proceed with open and hidden charm dynamics.

A. Perturbative treatment of D, $\bar{D}$ mesons and charmonia

The initial conditions for the production and subsequent propagation of D, $\bar{D}$ mesons and charmonia are incorporated in the HSD approach by a superposition of pp collisions described via scaled PYTHIA [32] simulations [27]. For the production and propagation of open and hidden charm hadrons, we employ a perturbative scheme as we did in Refs. [19,22,27]. Each perturbative particle h_i is produced in the transport calculation with a weight W_i given by the ratio of the actual production cross section divided by the inelastic nucleon-nucleon cross section, e.g.,

$$W_i = \frac{\sigma_{NN\to h_i+X}(s)}{\sigma_{NN}^{\text{inelas.}}(s)}. \tag{1}$$

We then follow the motion of the perturbative particles within the full background of strings/hadrons by propagating them as free hadrons, i.e., neglecting in-medium potentials, but we compute their collisional history with baryons and mesons or quarks and diquarks. The actual parametrizations of the total cross sections for D, D^*, D_s, D_s^* mesons as well as their antiparticles are given in Refs. [19,22,27] together with the cross sections for charmonium production in nucleon-nucleon and pion-nucleon collisions. The only modification introduced here relative to Refs. [19,22] is a change of the parametrization for the differential production cross section in transverse momentum. Our novel parametrization follows the first results from STAR [37] and is given by a power law in transverse momentum p_T

$$W(p_T) \sim \left(1 + \frac{p_T}{3.5}\right)^{-8.3}. \tag{2}$$

For simplicity and lack of further information, we assume that this parametrization holds for all D, $\bar{D}$ mesons as well as charmonia.

B. Cross sections involving charm hadrons

To study the effect of rescattering, we tentatively adopt the following dissociation cross sections of charmonia with baryons independent of the energy (in line with Refs. [19,22,27]):

$$\begin{aligned} \sigma_{c\bar{c}B} &= 6\,\text{mb}; \sigma_{J/\Psi B} = 4\,\text{mb}; \\ \sigma_{\chi_c B} &= 5\,\text{mb}; \sigma_{\Psi' B} = 5\,\text{mb}. \end{aligned} \tag{3}$$

In (3) the cross section $\sigma_{c\bar{c}B}$ stands for a (color dipole) preresonance ($c\bar{c}$) and baryon cross section, since the $c\bar{c}$ pair produced initially cannot be identified with a particular hadron due to the uncertainty relation in energy and time. For

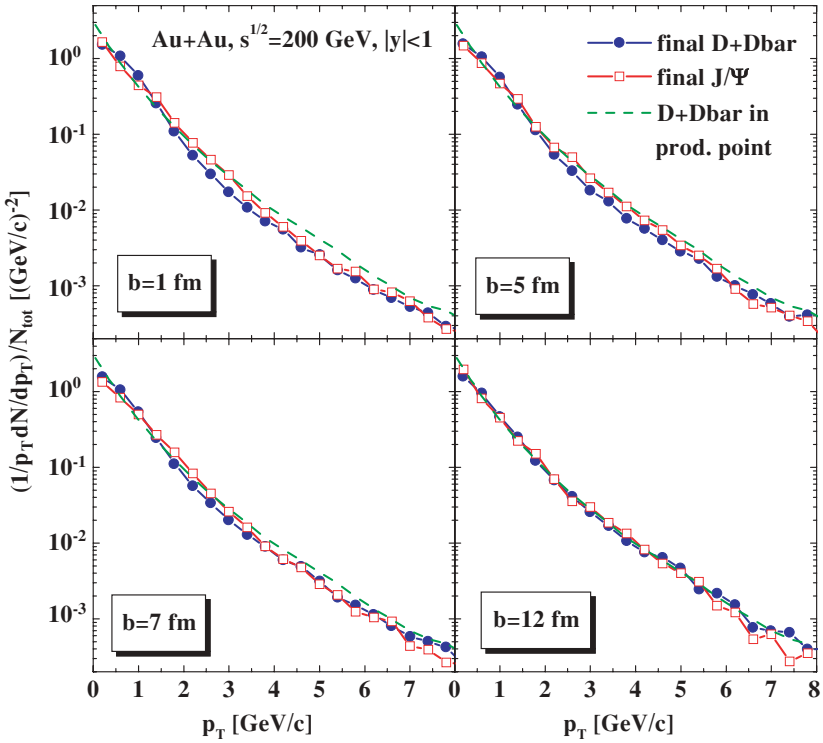

FIG. 1. (Color online) Transverse p_T spectra of the final $D + \bar{D}$ mesons (solid lines with full dots, blue) and J/Ψ (solid lines with open squares, red) from Au + Au collisions at $\sqrt{s} =$ 200 GeV calculated for $b = 1, 5, 7$, and 12 fm at midrapidity. The dashed lines correspond to the p_T spectra of D mesons at the production point.

the lifetime of the preresonance $c\bar{c}$ pair (in its rest frame) a value of $\tau_{c\bar{c}} = 0.3$ fm/c is assumed following Ref. [38]. This value corresponds to the mass difference of the Ψ' and J/Ψ.

For $D, D^*, \bar{D}, \bar{D}^*$-meson $(\pi, \eta, \rho, \omega)$ scattering, we address the calculations from Ref. [21,39], which predict elastic cross sections in the range of 10–20 mb depending on the size of the form factor employed. As a guideline we use a constant cross section of 10 mb for elastic scattering with mesons and also baryons, although the latter might be even higher for very low relative momenta.

The cross sections for charmonium production by open charm mesons or the inverse comover dissociation cross sections are not well known, and the significance of these channels is discussed controversially in the present literature (cf. Ref. [19] and references therein). Here we follow the simple two-body transition model introduced in Refs. [19,22] with a single free parameter, i.e., a matrix element squared M_0^2, that allows us to implement the backward reactions uniquely by employing detailed balance for each individual channel. The free matrix element was fixed in Ref. [22] in comparison to J/Ψ and Ψ' suppression data at SPS energies. For further details, we refer the reader to Refs. [19,22] in order to avoid unnecessary repetitions.

III. TRANSVERSE MOMENTUM SPECTRA

Because the results for charmonium suppression at SPS and RHIC energies—within the present approach—have been presented in Refs. [19,22], we directly continue with the transverse dynamics of open charm mesons and charmonia. In Fig. 1 we present the transverse p_T spectra of the final $D + \bar{D}$ mesons and J/Ψ from Au + Au collisions at $\sqrt{s} = 200$ GeV calculated for impact parameter $b = 1, 5, 7$, and 12 fm at midrapidity. The p_T spectra of D mesons at the production point are shown for reference, i.e., without any final-state interactions. For very peripheral Au + Au collisions, we find no effects from final-state interactions; whereas with increasing centrality, we see an enhancement of the spectra at low and moderate p_T from Au + Au collisions as well as a modest suppression at high p_T.

We note that the power-law parametrization (2) gives a substantial enhancement of the high-momentum tail of the open charm and charmonia p_T spectra compared to the previous parametrization used in HSD [19,22]. This is an improvement in the present approach as the new distribution provides a higher number of charm pairs at the beginning of the collisions. This will also affect the J/Ψ yield. Further experimental data on high p_T spectra in elementary as well as heavy ion collisions will fix the proper shape.

To quantify the effect of final-state interactions, we show in Fig. 2 the ratio of the final to the initial (i.e., at the production point) transverse p_T spectra of $D + \bar{D}$ mesons and J/Ψ from the same reaction for impact parameter $b = 1, 5, 7$, and 12 fm at midrapidity.

The actual ratios in Fig. 2 show an enhancement of $D, \bar{D}$ mesons at low momenta with a maximum at $p_T \approx 1$ GeV/c and a relative suppression for $p_T > 2$ GeV/c. These effects increase with the centrality of the Au + Au collision. For J/Ψ, a maximum in the ratio shows up at ~2 GeV/c, while it drops below 1 for $p_T >$ 3–4 GeV/c.

In accordance with the ratios in Fig. 2, the average value of the transverse momentum p_T, which is displayed in Fig. 3 at midrapidity for $D + \bar{D}$ mesons and J/Ψ, slightly increases (decreases) for J/Ψ ($D, \bar{D}$ mesons) with decreasing impact parameter b. The D-meson spectrum is relatively "hard" due

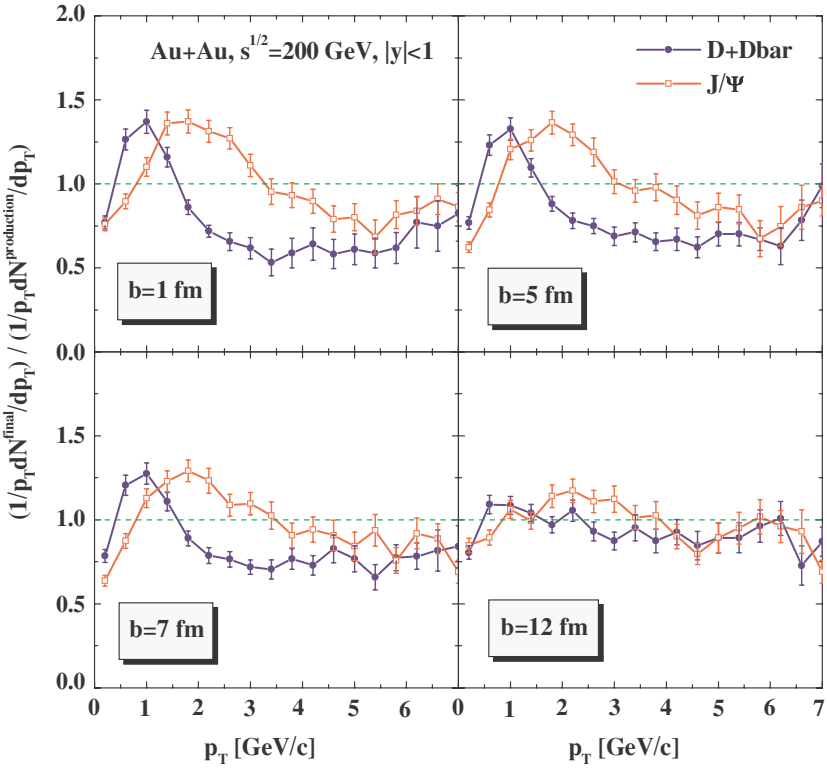

FIG. 2. (Color online) Ratio of the final to the initial (i.e., at the production point) transverse p_T spectra of $D + \bar{D}$ mesons (full dots, blue) and J/Ψ (open squares, red) from Au + Au collisions at $\sqrt{s} = 200$ GeV calculated for $b = 1$, 5, 7, and 12 fm at midrapidity.

to the large intrinsic charm quark mass. Through scatterings, the D mesons loose their energy at high p_T and develop the collective shoulder at low p_T. This explains the dropping of the D meson $\langle p_T \rangle$ in more central Au + Au collisions shown in Fig. 3. Such hadronic energy loss for D mesons will complicate the analysis of the gluon radiative energy loss before hadronization [40]. These main trends should be readily tested experimentally in the near future.

The question comes up how to interpret the findings in Figs. 1–3. We note that the maxima in the $D + \bar{D}$ and J/Ψ ratios disappear when switching off the rescattering with mesons in the transport approach. Thus, a collective acceleration of the $D + \bar{D}$ mesons occurs primarily via elastic scattering with

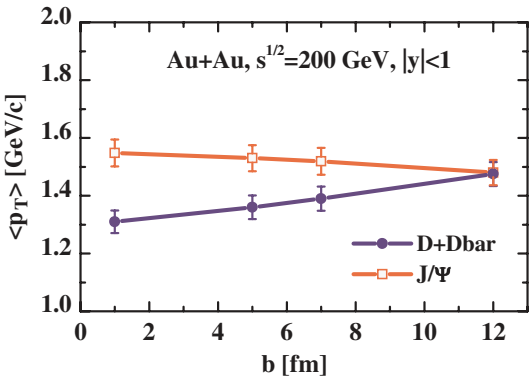

FIG. 3. (Color online) Average value of the transverse momentum p_T at midrapidity for D, $\bar{D}$ mesons (full dots, blue) and J/Ψ (open squares, red) from Au + Au collisions at $\sqrt{s} = 200$ GeV versus impact parameter b.

mesons. This argument does not hold at first sight for the J/Ψ's since their cross section with mesons is much lower, and no strong collective acceleration by rescattering should be expected [27]. The answer comes about as follows: As known from Refs. [19,22], the major fraction of final J/Ψ's stems from $D + \bar{D} \to J/\Psi(\chi_c) +$ meson channels and not from the primary production by NN collisions. This finding is quantified in Fig. 4, where the channel decomposition for the final J/Ψ's is shown as a function of the impact parameter b in Au + Au collisions at $\sqrt{s} = 200$ GeV. Except for peripheral reactions ($b > 9$ fm), the $D + \bar{D}$ channel dominates, while the production in initial baryon-baryon (BB) scattering supersedes all other reaction channels for the most peripheral reactions. The contribution from meson-baryon (mB) channels is low at all centralities.

We recall that the sensitivity of J/Ψ formation versus $D + \bar{D}$ annihilation to the formation amplitude has been studied in detail in Refs. [19,22]. The amplitudes for $D + \bar{D} \longleftrightarrow J/\Psi(\chi_c, \Psi') +$ mesons have been fitted to the experimental data on J/Ψ suppression and Ψ' to J/Ψ ratios at SPS energies and used also for the RHIC energies. This is legitimate because the latter reactions are typical comover reactions with low/moderate relative momenta. The average relative momenta for comover reactions do not change very much from top SPS to RHIC energies. At RHIC energies, however, the density of produced D mesons is much higher (17 $D + \bar{D}$ pairs in central collisions), and thus the probability to annihilate to charmonia ($\sim \rho^2$) is dramatically higher (cf. Fig. 6 in Ref. [22]). In fact, the system is close to chemical equilibrium in central reactions such that a sensitivity to the matrix elements is lost.

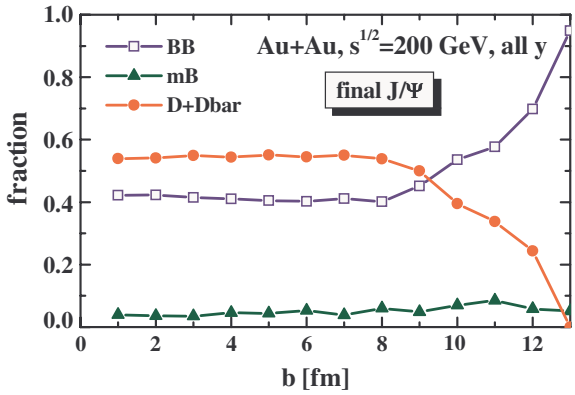

FIG. 4. (Color online) Channel decomposition for the final J/Ψ in Au + Au collisions at $\sqrt{s} = 200$ GeV within the transport approach as a function of the impact parameter b. The fraction of the final J/Ψ mesons produced in BB interactions is shown by the solid line with open squares (blue), the contribution from meson-baryon (mB) interactions is given in terms of the solid line with full triangles (green) and the $D\bar{D}$ annihilation fraction is displayed by the solid line with full circles (red).

According to Fig. 4, most of the J/Ψ's thus stem from $D + \bar{D}$ induced channels, and their production happens somewhat delayed in time when the $D, \bar{D}$ mesons have already picked up collective transverse momentum. In the $D + \bar{D} \rightarrow J/\Psi(\chi_c) +$ meson reaction, then, the formed J/Ψ carries the collective momentum of both D and $\bar{D}$ such that the charmonium appears to be accelerated even more than the D mesons. On the other hand, the J/Ψ's with a high transverse momentum (in the power-law tail) partly get dissociated with baryons of the target/projectile or with mesons in the expansion phase of the system. The probability of recreating a high p_T charmonium by the $D + \bar{D}$ channel is lower than in the initial NN channel since the invariant energy $\sqrt{s}$ in the $D + \bar{D}$ reaction is lower by more than an order of magnitude and exponential (thermal) J/Ψ spectra become populated. This interpretation will, furthermore, be supported by the studies in the next section.

IV. DIRECTED AND ELLIPTIC FLOW

Apart from the transverse flow that shows up as a "shoulder" in the p_T spectra at low momentum or a maximum in the ratio relative to pp spectra (cf. previous section), the directed flow

$$v_1(y, p_T) = \left\langle \frac{p_x}{p_T} \right\rangle_{y, p_T} \tag{4}$$

and the elliptic flow

$$v_2(y, p_T) = \left\langle \frac{p_x^2 - p_y^2}{p_T^2} \right\rangle_{y, p_T} \tag{5}$$

provide additional information on the collective currents of hadrons in the complex reaction [41].

Figure 5 shows the HSD predictions for the directed flow v_1 and elliptic flow v_2 of $D + \bar{D}$ mesons and J/Ψ from Au + Au collisions at $\sqrt{s} = 200$ GeV for $b = 7$ fm versus p_T for $0 < y < 1$ and rapidity y integrated over p_T. The directed flow v_1 is negative (within statistics up to $p_T = 3.5$ GeV/c) for both $D + \bar{D}$ mesons and J/Ψ's in the rapidity interval $0 < y < 1$. The tendency for v_1 of J/Ψ to be larger in magnitude for $0.5 < p_T < 2$ GeV/c supports the interpretation given in Sec. III that the final J/Ψ's primarily stem from $D + \bar{D}$ channels where both open charm mesons already have picked up some collective flow. The pronounced "antiflow" of open charm mesons and J/Ψ's becomes visible in the upper right panel of Fig. 5 where the slope dv_1/dy at midrapidity for

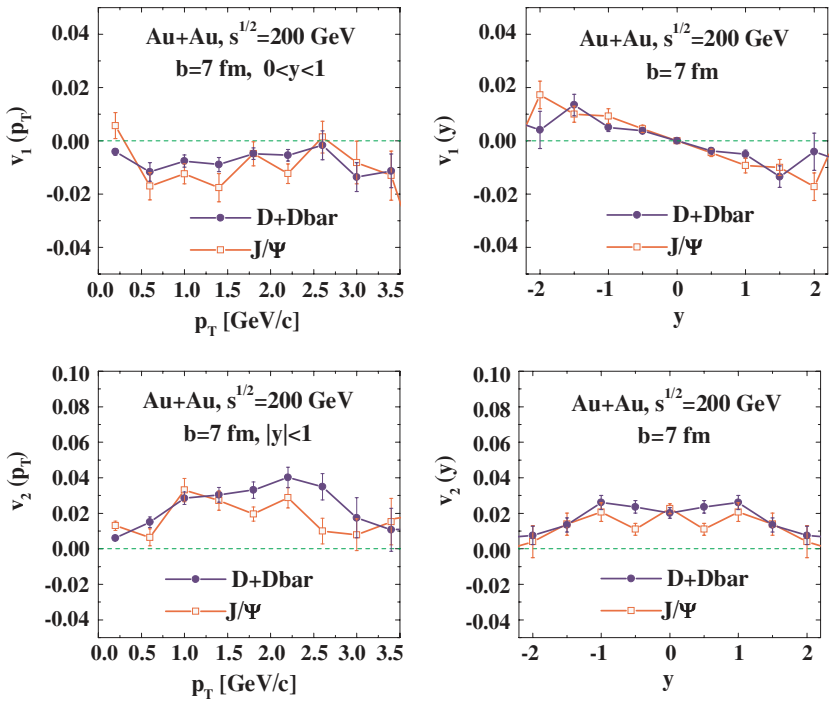

FIG. 5. (Color online) The directed flow v_1 (upper panels) and elliptic flow v_2 (lower panels) of $D + \bar{D}$ mesons (full dots, blue) and J/Ψ (open squares, red) from Au + Au collisions at $\sqrt{s} = 200$ GeV for $b = 7$ fm versus p_T for $0 < y < 1$ (left panels) and rapidity y (right panels) integrated over p_T.

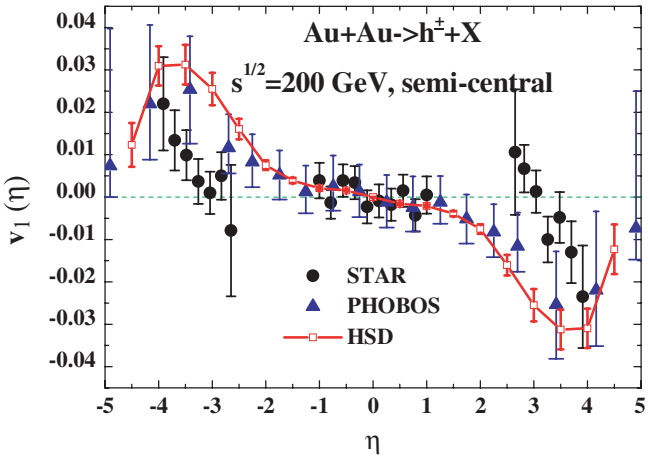

FIG. 6. (Color online) The directed flow v_1 for charged hadrons from semicentral Au + Au collisions at $\sqrt{s} = 200$ GeV versus pseudorapidity η in comparison to the data from STAR [37] (solid dots) and PHOBOS [42] (solid triangles).

J/Ψ's is also slightly larger in magnitude than that for $D + \bar{D}$ mesons.

The question now emerges of how most of the light hadrons flow in this reaction. The answer is given in Fig. 6, where the HSD result for the directed flow v_1 for charged hadrons from semicentral Au + Au collisions at $\sqrt{s} = 200$ GeV is plotted versus pseudorapidity η and compared to the data from the STAR Collaboration [37] and the PHOBOS Collaboration [42]. Apparently, the charged hadrons show a comparable flow $v_1(\eta)$ as the open charm mesons and charmonia; consequently, the latter flow with the bulk of the lighter hadrons made up from u, d, s and $\bar{u}, \bar{d}, \bar{s}$ quarks. We recall that the HSD calculations for the directed flow of charged hadrons match reasonably well with the data from Refs. [37,42] for $|\eta| < 3$ (cf. Ref. [43] for related Ultra-relativistic Quantum-Molecular Dynamics calculations).

Returning to the results for the elliptic flow v_2 in the lower panels of Fig. 5, we notice that both J/Ψ's and $D, \bar{D}$ mesons show in-plane flow since $v_2(y, p_T) > 0$. The elliptic flow of $D, \bar{D}$ mesons is larger for $1 < p_T < 3$ GeV/c than that of J/Ψ's, which indicates that the $D, \bar{D}$ mesons are accelerated earlier than the J/Ψ's. The elliptic flow v_2 shows a maximum around midrapidity as does the flow of charged hadrons [42] and is also slightly larger for $D, \bar{D}$ mesons than for J/Ψ's. However, for impact parameter $b = 7$ fm the elliptic flow of open charm mesons is $\leqslant 3\%$, whereas the elliptic flow of charged hadrons reaches up to $\sim 5\%$ at midrapidity. We recall that the HSD calculations underpredict the v_2 of charged hadrons at midrapidity by about 30–35% [19]. Consequently, one should also expect a larger elliptic flow for the open charm mesons and charmonia in experiment. We mention that in the quark coalescence model of Ref. [25], a significantly larger elliptic flow is obtained for both $D, \bar{D}$ mesons and J/Ψ.

We now turn to the multiplicity of $D, \bar{D}$ mesons and J/Ψ versus centrality in Au + Au collisions at $\sqrt{s} = 200$ GeV. The left part of Fig. 7 shows the multiplicity of $D + \bar{D}$ pairs and J/Ψ from Au + Au collisions at $\sqrt{s} = 200$ GeV integrated over rapidity versus impact parameter b, whereas the right part displays the ratio of the multiplicities of J/Ψ over $D + \bar{D}$ pairs versus b. Note that the J/Ψ multiplicity on the left-hand side has been multiplied by a factor of 100. Whereas we expect ~ 17 $D + \bar{D}$ pairs in the top central collisons, the J/Ψ multiplicity is only $\sim 5 \times 10^{-2}$, i.e., lower by a factor of ~ 300.

The right-hand side of Fig. 7 shows the ratio of the multiplicity of final J/Ψ's over $D + \bar{D}$ pairs versus impact parameter b. Since the multiplicity of $D + \bar{D}$ pairs scales directly with the number of binary (initial) NN collisions in the HSD transport approach [27], this ratio gives information about J/Ψ suppression relative to binary scaled pp collisions. We find that in accordance with the previous studies [19,22] the J/Ψ suppression in very central collisions relative to very peripheral reactions is a factor of ~ 2.5. Note that the explicit shape of this ratio versus b is the result of a complex coupled-channel problem that cannot be anticipated by simple scaling arguments. We recall that the dominant charmonium absorption channel in our transport calculations is the very early color-dipole dissociation with nucleons of the target/projectile (or their baryon-like remnants). These early dissociation reactions involve a high invariant collision energy such that the final fragments are distributed in a wide rapidity range which makes any recombination back to the original color-dipole–nucleon channel very unlikely. The formation of charmonium states (as well as $D, \bar{D}$ mesons) occurs later with characteristic formation times of 0.3 and 0.5 fm/c in their rest frame, respectively. Moreover, any dissociation with mesons is delayed until the latter have formed (cf. [19]). Now the dissociation of charmonia with comoving hadrons is compensated to a large extent by the inverse $D + \bar{D} \rightarrow$

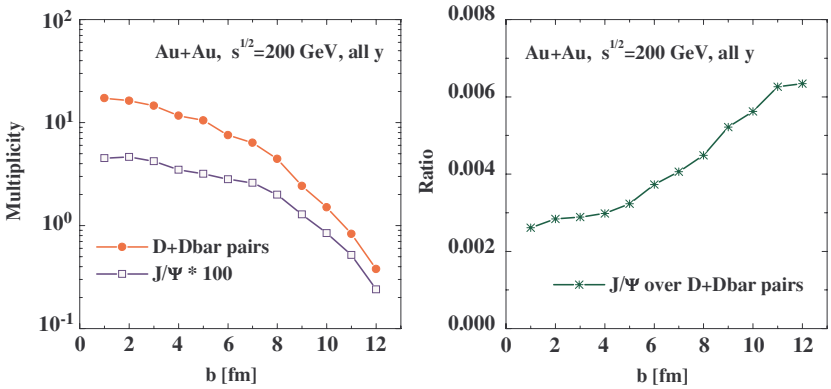

FIG. 7. (Color online) Left panel: multiplicity of $D + \bar{D}$ pairs (full dots, red) and J/Ψ ($\times 100$, open squares, blue) from Au + Au collisions at $\sqrt{s} = 200$ GeV integrated over rapidity versus impact parameter b. Right panel: ratio of the multiplicity of J/Ψ over $D + \bar{D}$ pairs versus b.

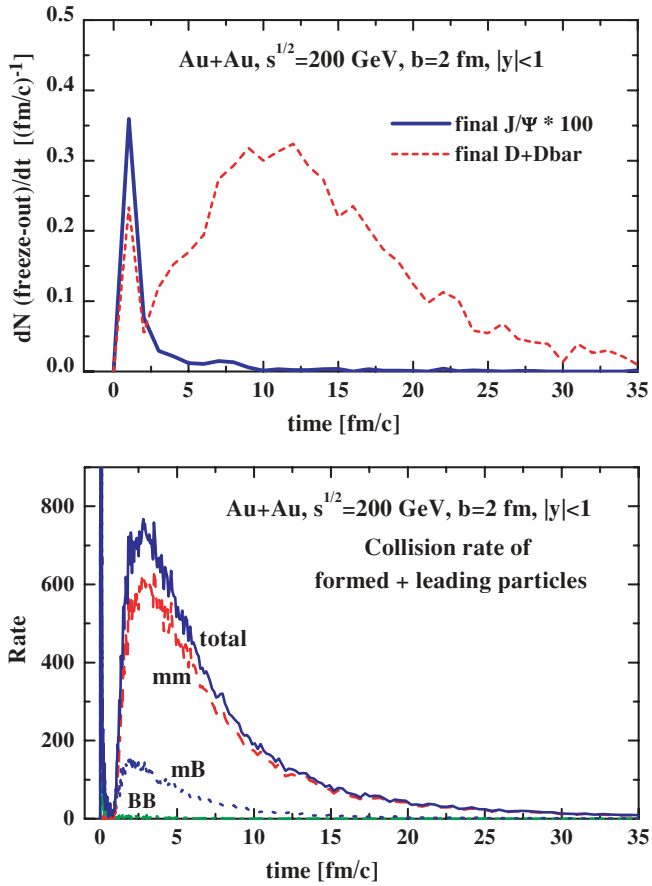

FIG. 8. (Color online) Upper panel: distribution in time of the last interaction for the final J/Ψ mesons ($\times 100$, solid line, blue) and $D + \bar{D}$ mesons (dashed line, red) from Au + Au collisions for $b = 2$ fm at $\sqrt{s} = 200$ GeV ($|y| \leqslant 1$). Lower panel: time evolution of the collision rate of formed and leading particles from BB, mB, and mm collisions from Au + Au collisions for $b = 2$ fm at $\sqrt{s} = 200$ GeV integrated over rapidity.

charmonium + meson channels at top RHIC energies. The actual time-integrated reaction rates for the forward and backward channels are shown in Fig. 5 of [22] versus centrality. Since both reaction channels turn out to be comparable in the time-integrated rate for midcentral and central collisions, the net result is not evident *a priori*. We recall that the J/Ψ's gain slightly from the $D + \bar{D}$ channels whereas the χ_c and Ψ' states loose from the dissociation channels with mesons (cf. Fig. 6 in [22]). Now the feeddown from χ_c and Ψ' to J/Ψ's has to be included for the final J/Ψ multiplicity, which for Au + Au at top RHIC energies shows a small net suppression from comover reactions on top of the early suppression by interactions with projectile/target nucleons. This rather complicated coupled-channel scenario finally leads to the ratio of J/Ψ over $D + \bar{D}$ pairs in Fig. 7.

We now turn to the freeze-out properties of $D + \bar{D}$ mesons and J/Ψ's. The upper panel of Fig. 8 presents the distribution in time of the last interaction for the final J/Ψ mesons and $D + \bar{D}$ mesons from Au + Au collisions for $b = 2$ fm at $\sqrt{s} =$ 200 GeV at midrapidity ($|y| \leqslant 1$). The production time was also recorded if the particles did not suffer from a further interaction (initial peaks up to 2 fm/c). The time $t = 0$ is defined by the contact time of the heavy ions. Whereas the J/Ψ mesons freeze-out early due to their small cross section with light hadrons, the $D + \bar{D}$ mesons interact for a long time and freeze-out on average at 10–12 fm/c.

The lower panel of Fig. 8 shows the collision rate of formed and leading particles from baryon-baryon (BB), meson-baryon (mB), and meson-meson (mm) collisions from Au + Au collisions at $b = 2$ fm and $\sqrt{s} = 200$ GeV integrated over rapidity. Here leading diquarks are counted as baryons (B) whereas leading quarks and antiquarks are registered as mesons (m). The rate of BB collisions shows a strong peak during the passage time of the heavy ions (<0.2 fm/c) and is almost negligible later. The mB collision rate (apart from the initial peak for $t < 0.2$ fm/c) shows a sizable contribution only after a short time delay of $\sim$1 fm/c, which is the scale of the hadron formation time for low momenta in the c.m. system. We point out that the very early mB collisions ($t <$ 0.4 fm/c) correspond to prehadron interactions, where a quark from a struck nucleon—forming an endpoint of the excited string—interacts without time delay (cf. Ref. [44] for a detailed discussion of the prehadron concept in HSD). Furthermore, the early interactions of formed mesons (for $1 < t < 4$ fm/c) occur mostly in the outer transverse region of the initial fireball where the energy density is below 1 GeV/fm^3.

As seen from Fig. 8, the mm collision rate of formed mesons also starts with a short delay in the order of the formation time τ_f but supersedes the mB collision rate by more than a factor of 4. The maximum in the mm collision rate occurs for $t \approx 3$–4 fm/c when the energy density in a sizable volume drops below 1 GeV/fm^3 and the system is still very dense. We point out, furthermore, that the "hadronic burning" by meson-baryon and meson-meson collisions persists up to rather long times since bunches of close-by hadrons may interact almost continuously if their relative momenta are low.

When comparing the two graphs in Fig. 8, we notice that the maximum in the mm collision rate occurs much earlier than the average freeze-out of $D + \bar{D}$ mesons (at 9–12 fm/c). This further supports our conjecture stated at the end of Sec. III that the $D + \bar{D}$ mesons suffer a couple of interactions with the light mesons and pick up collective flow before they freeze-out rather late on a time scale that is comparable to the freeze-out time for light hadrons if one discards the very late decay of resonances (e.g., $\omega \to 3\pi$, $\Delta \to N\pi$, $K^* \to K\pi$, etc.).

V. SUMMARY

In this work, we extended our previous investigations within the HSD transport approach in Refs. [19,22,27] with respect to the collective dynamics of D, $\bar{D}$ mesons and charmonia. Our detailed studies of Au + Au collisions at $\sqrt{s} = 200$ GeV have shown that

- Prehadronic and hadronic interactions generate a transverse collective flow of D, $\bar{D}$ mesons and charmonia that shows up as a shoulder in the low-momentum spectra or as a maximum in the ratio relative to scaled pp collisions.
- The high p_T power-law tail of the spectra is only moderately suppressed.

- The directed flow of $D, \bar{D}$ mesons and charmonia is comparable to that of the light charged hadrons.
- The elliptic flow of $D, \bar{D}$ mesons and charmonia is smaller than that of the light hadrons.
- The $D, \bar{D}$ mesons freeze-out on average at $\sim 9-12$ fm/c, which is comparable to the freeze-out time for light hadrons (when neglecting explicit resonance decays).

Whereas the collective acceleration of the $D + \bar{D}$ mesons via elastic scattering with mesons in the expansion phase of the "fireball" can be well understood on the basis of the rather large cross section of $D, \bar{D}$ mesons with nucleons and mesons [21,39]—in view of the light quark/antiquark content of these states—the collective dynamics of the J/Ψ's cannot be explained in this way because the J/Ψ cross section with mesons is much lower. However, the dominant fraction ($>50\%$) of final J/Ψ's in central and midcentral reactions stems from $D + \bar{D} \rightarrow J/\Psi(\chi_c) +$ meson channels and to a lesser extent from the primary production by NN collisions (cf. Fig. 4). Thus, the production of the final charmonia is delayed in time until after the $D, \bar{D}$ mesons have picked up collective flow from interactions with light (and fast) hadrons. Furthermore, in the $D + \bar{D} \rightarrow J/\Psi(\chi_c) +$ meson reaction, the formed J/Ψ carries the collective momentum of both D and $\bar{D}$ such that the charmonium appears to be accelerated even more than the D mesons (cf. Figs. 2 and 5). On the other hand, the elliptic flow of $D, \bar{D}$ mesons is slightly larger than that of J/Ψ's, which indicates on average an earlier production of the open charm mesons.

The differential spectra and ratios as well as the differential flow analysis for $v_1(y, p_T)$ and $v_2(y, p_T)$ for open charm hadrons and charmonia are expected to be proven/disproven in the near future by the RHIC experiments. Our analysis and interpretation of the results have also paved the way for extracting relevant time scales and possibly interaction rates or freeze-out times. Sensible deviations from our predictions will point toward a dynamical origin that is not included in our present calculations and should be addressed to explicit partonic interactions in a possibly colored medium.

ACKNOWLEDGMENTS

The authors thank M. Bleicher, P. Braun-Munzinger, A. P. Kostyuk, A. Mishra, J. Schaffner-Bielich, and L. Tolos for valuable discussions. E.L.B. was supported by DFG and GSI. N.X. was supported by the U.S. Department of Energy under Contract No. DE-AC03-76SF00098.

[1] H. Stöcker and W. Greiner, Phys. Rep. **137**, 277 (1986).
[2] W. Cassing and U. Mosel, Prog. Part. Nucl. Phys. **25**, 235 (1990).
[3] W. Cassing and E. L. Bratkovskaya, Phys. Rep. **308**, 65 (1999).
[4] *Quark Matter 2002*, Nucl. Phys. **A715**, 1 (2003); *Quark Matter 2004*, J. Phys. G **30**, S633 (2004).
[5] *Strange Quark Matter 2003*, J. Phys. G **30**, 1 (2004).
[6] T. Matsui and H. Satz, Phys. Lett. **B178**, 416 (1986).
[7] H. Satz, Rep. Prog. Phys. **63**, 1511 (2000).
[8] S. Datta, F. Karsch, P. Petreczky, and I. Wetzorke, J. Phys. G **30**, S1347 (2004).
[9] M. Asakawa and T. Hatsuda, J. Phys. G **30**, S1337 (2004).
[10] F. Karsch, J. Phys. G **30**, S889 (2004).
[11] P. Braun-Munzinger and J. Stachel, Phys. Lett. **B490**, 196 (2000); Nucl. Phys. **A690**, 119c (2001).
[12] M. I. Gorenstein, A. P. Kostyuk, H. Stöcker, and W. Greiner, Phys. Lett. **B509**, 277 (2001); J. Phys. G **27**, L47 (2001).
[13] A. P. Kostyuk, M. I. Gorenstein, H. Stöcker, and W. Greiner, Phys. Lett. **B531**, 195 (2002).
[14] A. P. Kostyuk, M. I. Gorenstein, H. Stöcker, and W. Greiner, J. Phys. G **28**, 2297 (2002).
[15] R. L. Thews, M. Schroedter, and J. Rafelski, Phys. Rev. C **63**, 054905 (2001).
[16] W. Cassing, Nucl. Phys. **A700**, 618 (2002).
[17] P. Braun-Munzinger, J. Stachel, and C. Wetterich, Phys. Lett. **B596**, 61 (2004).
[18] Z. Xu and C. Greiner, hep-ph/0406278.
[19] E. L. Bratkovskaya, W. Cassing, and H. Stöcker, Phys. Rev. C **67**, 054905 (2003).
[20] L. Grandchamp and R. Rapp, Phys. Lett. **B523**, 60 (2001); Nucl. Phys. **A709**, 415 (2002).
[21] Z. Lin and C. M. Ko, J. Phys. G **27**, 617 (2001); Z. W. Lin and C. M. Ko, Phys. Rev. C **65**, 034904 (2002).
[22] E. L. Bratkovskaya, A. P. Kostyuk, W. Cassing, and H. Stöcker, Phys. Rev. C **69**, 054903 (2004).
[23] A. Dumitru and C. Spieles, Phys. Lett. **B446**, 326 (1999).
[24] N. Xu, Prog. Part. Nucl. Phys. **53**, 165 (2004), and references therein.
[25] V. Greco, C. M. Ko, and R. Rapp, Phys. Lett. **B595**, 202 (2004).
[26] Z. W. Lin and D. Molnar, Phys. Rev. C **68**, 044901 (2003).
[27] W. Cassing, E. L. Bratkovskaya, and A. Sibirtsev, Nucl. Phys. **A691**, 753 (2001).
[28] I. G. Bearden *et al.* (NA44 Collaboration), Phys. Rev. Lett. **78**, 2080 (1997).
[29] H. van Hecke, H. Sorge, and N. Xu, Phys. Rev. Lett. **81**, 5764 (1998).
[30] J. Geiss, W. Cassing, and C. Greiner, Nucl. Phys. **A644**, 107 (1998).
[31] H. Pi, Comput. Phys. Commun. **71**, 173 (1992).
[32] H.-U. Bengtsson and T. Sjöstrand, Comput. Phys. Commun. **46**, 43 (1987).
[33] Z. W. Lin *et al.*, Nucl. Phys. **A698**, 375 (2002).
[34] S. A. Bass, B. Müller, and D. K. Srivastava, J. Phys. G **30**, S1283 (2004).
[35] H. Weber, E. L. Bratkovskaya, W. Cassing, and H. Stöcker, Phys. Rev. C **67**, 014904 (2003).
[36] E. L. Bratkovskaya, *et al.*, Phys. Rev. C **69**, 054907 (2004).
[37] An Tai *et al.* (STAR Collaboration), J. Phys. G **30**, S809 (2004).
[38] D. Kharzeev and R. L. Thews, Phys. Rev. C **60**, 041901 (1999).
[39] Z. Lin and C. M. Ko, Phys. Rev. C **62**, 034903 (2000).
[40] Y. L. Dokshitzer and D. E. Kharzeev, Phys. Lett. **B519**, 199 (2001); M. Djordjevic and M. Gyulassy, J. Phys. G **30**, S1183 (2004).
[41] H. Stöcker, Nucl. Phys. **A750**, 121 (2005).
[42] S. Manly *et al.* (PHOBOS Collaboration), nucl-ex/0405029.
[43] M. Bleicher and H. Stöcker, Phys. Lett. **B526**, 309 (2002).
[44] W. Cassing, K. Gallmeister, and C. Greiner, Nucl. Phys. **A735**, 277 (2004).